CAMBRIDGE
UNIVERSITY PRESS

Article

Davidbrownite-(NH$_4$), (NH$_4$,K)$_5$(V^{4+}O)$_2$(C$_2$O$_4$)[PO$_{2.75}$(OH)$_{1.25}$]$_4$·3H$_2$O, a new phosphate–oxalate mineral from the Rowley mine, Arizona, USA

Anthony R. Kampf[1]* 🔾, Mark A. Cooper[2], George R. Rossman[3], Barbara P. Nash[4], Frank. C. Hawthorne[2] and Joe Marty[5]

[1]Mineral Sciences Department, Natural History Museum of Los Angeles County, 900 Exposition Boulevard, Los Angeles, California 90007, USA; [2]Department of Geological Sciences, University of Manitoba, Winnipeg, Manitoba, R3T 2N2, Canada; [3]Division of Geological and Planetary Sciences, California Institute of Technology, Pasadena, California 91125, USA; [4]Department of Geology and Geophysics, University of Utah, Salt Lake City, Utah 84112, USA; and [5]5199 East Silver Oak Road, Salt Lake City, Utah 84108, USA

Abstract

Davidbrownite-(NH$_4$), (NH$_4$,K)$_5$(V^{4+}O)$_2$(C$_2$O$_4$)[PO$_{2.75}$(OH)$_{1.25}$]$_4$·3H$_2$O, is a new mineral species from the Rowley mine, Maricopa County, Arizona, USA. It occurs in an unusual bat-guano-related, post-mining assemblage of phases that include a variety of vanadates, phosphates, oxalates and chlorides, some containing NH$_4^+$. Other secondary minerals found in association with davidbrownite-(NH$_4$) are antipinite, fluorite, mimetite, mottramite, quartz, rowleyite, salammoniac, struvite, vanadinite, willemite and wulfenite. Crystals of davidbrownite-(NH$_4$) are light green–blue needles or narrow blades up to ∼0.2 mm long. The streak is white, the lustre is vitreous, Mohs hardness is *ca.* 2, tenacity is brittle and fracture is splintery. There are two good cleavages in the [010] zone, probably {100} and {001}. The measured density is 2.12(2) g cm^{-3}. Davidbrownite-(NH$_4$) is optically biaxial (+) with α = 1.540(2), β = 1.550(5) and γ = 1.582(2) (white light); 2V = 58.5(5)°; moderate *r* > *v* dispersion; and orientation *Z* = **b** and *Y* ≈ **a**. Pleochroism: *X* = pale blue, *Y* = nearly colourless, *Z* = light blue; and *Y* < *X* < *Z*. Electron microprobe analysis gave the empirical formula [(NH$_4$)$_{3.11}$K$_{1.73}$Na$_{0.09}$]$_{\Sigma 4.93}$[(V$^{4+}_{1.92}$Mg$_{0.01}$Al$_{0.02}$)$_{\Sigma 1.95}$O$_2$](C$_2$O$_4$) [(P$_{3.94}$As$_{0.12}$)$_{\Sigma 4.06}$O$_{10.94}$ (OH)$_{5.06}$]·3H$_2$O, with the C and H content provided by the crystal structure. Raman and infrared spectroscopy confirmed the presence of NH$_4$ and C$_2$O$_4$. Davidbrownite-(NH$_4$) is monoclinic, *P*2$_1$/*c*, with *a* = 10.356(6), *b* = 8.923(5), *c* = 13.486(7) Å, β = 92.618(9)°, *V* = 1244.9(12) Å^3 and *Z* = 2. The crystal structure of davidbrownite-(NH$_4$) (*R*$_1$ = 0.0524 for 2062 *I*$_o$ > 2σ*I* reflections) consists of a chain structural unit with the formula {(V^{4+}O)$_2$(C$_2$O$_4$)[PO$_{2.75}$(OH)$_{1.25}$]$_4$}$^{5-}$, and a disordered interstitial complex containing five large monovalent cations (NH$_4^+$ and K$^+$) and three H$_2$O groups pfu. Strong hydrogen bonds form links within and between the chains.

Introduction

In our investigations of post-mining mineralisation in mines of the southwestern United States, we encountered an unusual and still actively forming bat-guano assemblage at depth (125 feet) in the Rowley mine near Theba, Arizona. Previously, from this assemblage, we reported on the new mineral rowleyite, [Na(NH$_4$,K)$_9$Cl$_4$] [V$^{5+,4+}_2$(P,As)O$_8$]$_6$·*n*[H$_2$O,Na,NH$_4$,K,Cl], which has a microporous vanadate–phosphate framework structure (Kampf *et al.*, 2017) and the new mineral phoxite, (NH$_4$)$_2$Mg$_2$(C$_2$O$_4$)(PO$_3$OH)$_2$(H$_2$O)$_4$, which is the first mineral found to contain both phosphate and oxalate groups (Kampf *et al.*, 2019). Herein, we report on the new mineral davidbrownite-(NH$_4$), (NH$_4$,K)$_5$(V^{4+}O)$_2$(C$_2$O$_4$) [PO$_{2.75}$(OH)$_{1.25}$]$_4$·3H$_2$O, which is the second mineral containing both phosphate and oxalate groups and which has a novel structure that includes multiple strong hydrogen bonds.

The name davidbrownite-(NH$_4$) honours British–Canadian crystallographer Dr. I. David Brown (born April 11, 1932) in

Edgeware, Middlesex, UK. Dr. Brown did his PhD at the Royal Institution of Great Britain and Eidgenössische Technische Hochschule (ETH) Zürich, before moving in 1959 to McMaster University, Hamilton, Ontario, Canada, for a post-doctoral position. Following his post-doctoral years, Dr. Brown joined the Physics Department (now the Department of Physics and Astronomy) at McMaster where he has stayed for his entire professional career, and is now Professor Emeritus. Dr. Brown is well known for developing Bond-Valence Theory (Brown, 2002, 2016), which is used extensively by mineralogical crystallographers the world over to both validate structural arrangements derived from crystal-structure solution and refinement, and to derive many crystal-chemical details (e.g. the presence of hydrogen and its speciation in structures, the arrangements of hydrogen bonds) that are not revealed directly by crystal-structure refinement. Dr. Brown has given his permission for this mineral to be named in his honour. For naming and species definition, the total occupancy of the three large cation sites in the structure is employed; thereby, the '-(NH$_4$)' suffix in the name reflects the fact that NH$_4^+$ > K$^+$. If an analogue with K$^+$ > NH$_4^+$ were found, it would be named davidbrownite-(K).

The new mineral and name were approved by the Commission on New Minerals, Nomenclature and Classification of the International Mineralogical Association (IMA2018-129, Kampf *et al.*, 2019b). Three small cotype specimens are deposited in

the collections of the Natural History Museum of Los Angeles County, Los Angeles, California, USA, catalogue numbers 66951, 66955 and 66959.

Occurrence

Davidbrownite-(NH_4) was found on the 125-foot level of the Rowley mine, ~20 km NW of Theba, Maricopa County, Arizona, USA (33°2′57″N 113°1′49.59″W). The Rowley mine (in the Painted Rock mining district) is a former Cu–Pb–Au–Ag–Mo–V–baryte–fluorite mine that exploited veins presumed to be related to the intrusion of an andesite porphyry dyke into Tertiary volcanic rocks. Although the mine has not been operated for ore since 1923, collectors took notice of the mine as a source of fine wulfenite crystals around 1945. The most detailed recent account of the history, geology and mineralogy of the mine was by Wilson and Miller (1974).

The new mineral occurs in a hot and humid area of the mine in an unusual bat-guano-related, post-mining assemblage of phases that include a variety of vanadates, phosphates, oxalates and chlorides, some containing NH_4^+. This secondary mineral assemblage is found growing on baryte–quartz-rich matrix and, besides davidbrownite-(NH_4) includes antipinite, fluorite, mimetite, mottramite, phoxite (Kampf *et al.*, 2019a), quartz, rowleyite (Kampf *et al.*, 2017), salammoniac, struvite, vanadinite, willemite, wulfenite and several other potentially new minerals.

Physical and optical properties

Crystals of davidbrownite-(NH_4) are needles or narrow blades, up to ~0.2 mm long, usually growing in sprays (Fig. 1). The blades are elongate on [010], more or less flattened on {100} and exhibit the crystal forms {100}, {001} and {230} (Fig. 2). No twinning was observed. The colour is light green blue (close to Pantone 317 C), the streak is white, the lustre is vitreous, the Mohs hardness is ~2, the tenacity is brittle and the fracture is splintery. There are two good cleavages in the [010] zone, probably {100} and {001}. The density measured by flotation in a mixture of methylene iodide and toluene is 2.12(2) g cm^{-3}. The calculated density is 2.107 g cm^{-3} using the empirical formula and 2.116 g cm^{-3} using the ideal formula. Davidbrownite-(NH_4) is non-fluorescent in longwave and shortwave ultraviolet light. The mineral is insoluble at room temperature in H_2O, but easily soluble in dilute HCl.

Davidbrownite-(NH_4) is optically biaxial (+) with $\alpha = 1.540(2)$, $\beta = 1.550(5)$ and $\gamma = 1.582(2)$ determined in white light. The 2V measured using extinction data with *EXCALIBR* (Gunter *et al.*, 2004) is 58.5(5)° and the calculated 2V is 59.4°. Moderate $r > v$ dispersion was observed. The optical orientation is $Z = \mathbf{b}$ and $Y \approx \mathbf{a}$. Pleochroism is distinct: X = pale blue, Y = nearly colourless and Z = light blue; $Y < X < Z$.

Raman and ATR-IR spectroscopy

The Raman spectrum (Fig. 3) was recorded using a Renishaw M1000 micro-Raman spectrometer with a 514.5 nm green laser, with ~1 μm diameter beam and with 2 mW on the unoriented sample. The attenuated total reflectance (ATR) infrared (IR) spectrum (Fig. 4) was recorded using a SensIR Durascope ATR accessory with a Thermo-Nicolet iS50 FTIR spectrometer on a small amount of powdered material.

Weak Raman bands and a stronger infrared band in the 1700–1600 cm^{-1} region, as seen in the davidbrownite-(NH_4) spectra, are
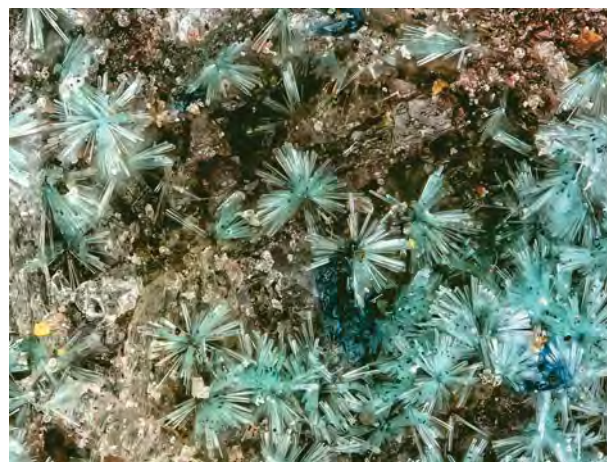

Fig. 1. Sprays of davidbrownite-(NH_4) needles with deep blue antipinite on quartz–baryte matrix; Field of view 1.14 mm. Specimen number 66951.

consistent with the spectroscopic features of oxalate groups in potassium manganese oxalotophosphite (Orive *et al.*, 2018), ammonium vanadyl oxalatophosphite (Kouvatas *et al.*, 2017) and various minerals with essential (Frost and Weier, 2003) and non-essential (Chukanov *et al.*, 2011) oxalate. The strong Raman band at 1499 cm^{-1} corresponds to the strong C–O stretch seen in other oxalates such as the 1496 cm^{-1} band in potassium–oxalate solution (Edwards *et al.*, 1991), which also has a less-intense 1459 cm^{-1} band comparable to the 1453 cm^{-1} band in the davidbrownite-(NH_4) spectra.
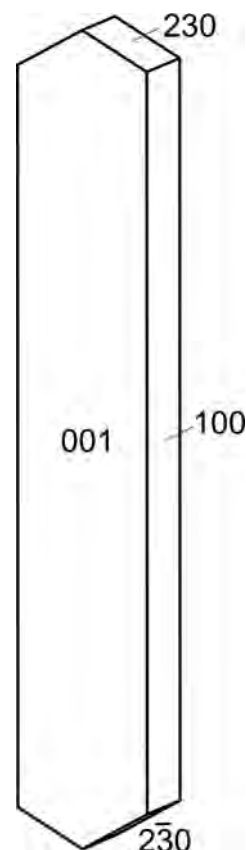

Fig. 2. Crystal drawing of davidbrownite-(NH_4); clinographic projection in a non-standard orientation, **b** vertical.
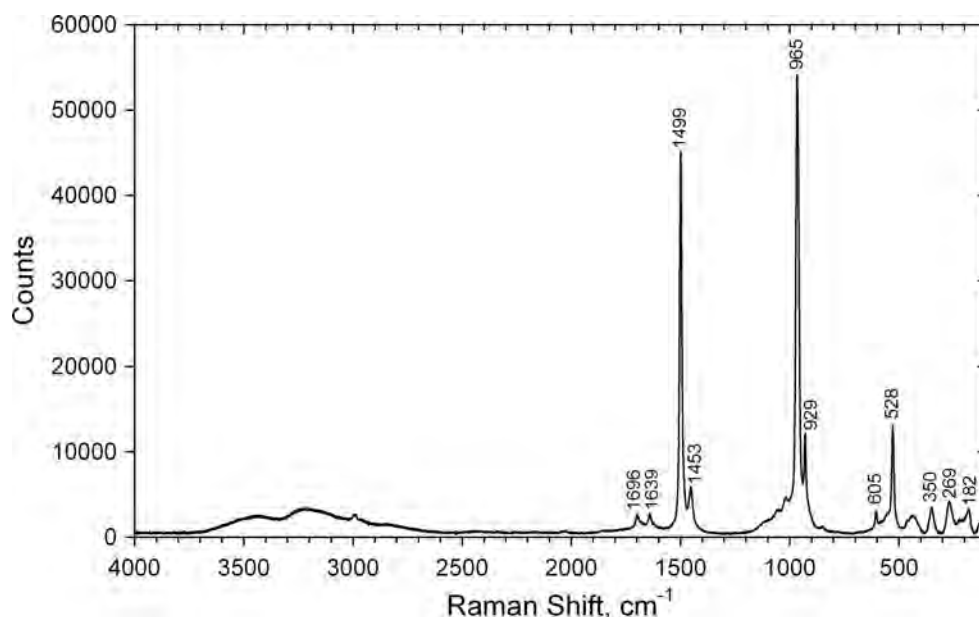
Fig. 3. Raman spectrum of davidbrownite-(NH$_4$).

Ammonium features are commonly observed in the 3600–2800 cm^{-1} range that overlaps the OH stretching region (Beran *et al.*, 1992). Davidbrownite-(NH$_4$) has several IR absorption and Raman features in this region; however, without detailed deuteration studies of synthetic material, definitive distinction of NH$_4$ and OH features in this and other regions is not possible. The IR band at 1429 cm^{-1} is consistent with NH$_4$ deformation.

Phosphate bands commonly occur between 1100 and 1000 cm^{-1}, as noted for vanadyl oxalatophosphate (Kouvatas *et al.*, 2017), and these authors assigned V = O stretching to a band at 973 cm^{-1}. Comparable features are seen in these regions of the davidbrownite-(NH$_4$) spectra.

The structure of davidbrownite-(NH$_4$) (see below) suggests that there are probably strong hydrogen bonds (short O–O

distances). Using the O–O distances from the structure refinement and the band positions from fig. 1 of Libowitzky (1999), estimated approximate infrared band positions for the hydrogen-bonded OH units can be derived (Table 1). Low energy features from strong hydrogen bonds tend to give broad infrared bands (Hammer *et al.*, 1998). Several of the possible weak hydrogen bonds are consistent with spectral features in the 3500–3200 cm^{-1} region, but with the exception of the 3428 cm^{-1} feature, do not correspond well with the approximate predictions. The strong hydrogen bond predicted to be in the 1680 cm^{-1} region is near the 1650 cm^{-1} band, but this band position is appropriate for the oxalate antisymmetric stretching mode and is extremely narrow compared to strong OH bands at such low wavenumbers. Clear evidence of the other two strong hydrogen bonds in the
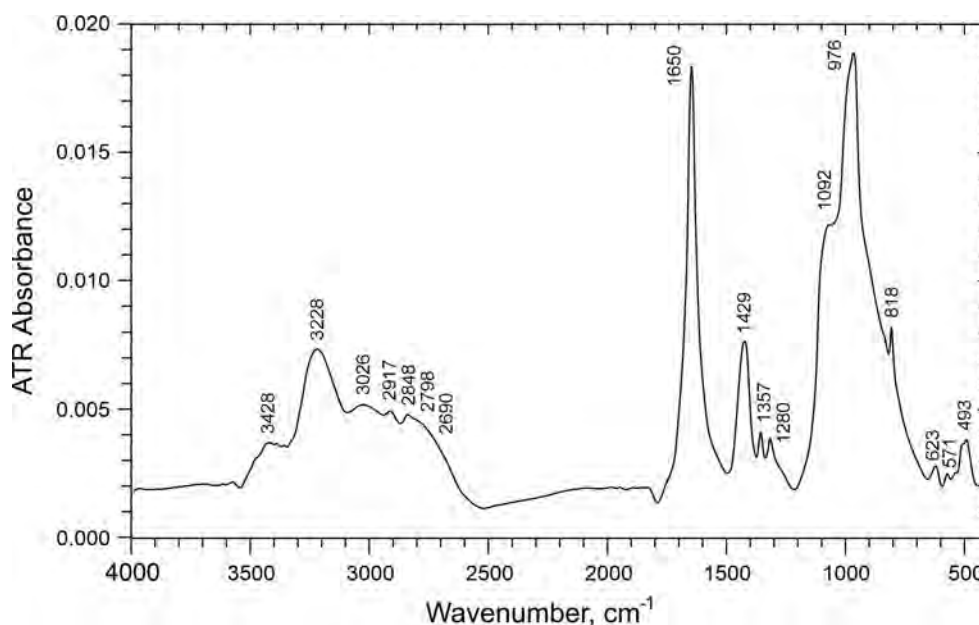

Fig. 4. ATR-IR spectrum of davidbrownite-(NH$_4$).

Table 1. Predicted O···H absorption bands from the possible hydrogen-bond O_{donor}–$O_{acceptor}$ distances.

O–O distance (in Å)	Wavenumbers (in cm^{-1})	
	Predicted*	Observed
Likely strong hydrogen bonds		
2.469	1325	unlikely
2.500	1680	1650
2.573	2525	none
Possible weak hydrogen bonds		
2.727	3280	3228
2.780	3330	none
2.825	3430	3428
2.920	3510	none
2.993	3550	none

*See table 1 of Libowitzky (1999).

predicted positions is not apparent from the infrared spectrum, although the weak absorption in the 1700–2500 cm^{-1} region could possibly be from hydrogen-bonded OH acidphosphate groups.

Chemical analysis

Electron probe microanalyses (EPMA) of davidbrownite-(NH$_4$) (four points) were undertaken at the University of Utah on a Cameca SX-50 electron microprobe with four wavelength dispersive spectrometers using *Probe for EPMA* software. Analytical conditions were 15 kV accelerating voltage, 10 nA beam current and beam diameters of 5 and 10 μm. Raw X-ray intensities were corrected for matrix effects with a φρ(z) algorithm (Pouchou and Pichoir, 1991). Intensities for Na, K and P were corrected for time-dependent variation in intensity during analyses. The crystals fragmented when polished, so the analyses were done on unpolished but smooth crystal faces. Because insufficient material is available for a direct determination of H (H$_2$O) or C (C$_2$O$_3$), they were calculated on the basis of the structure determination. The high analytical total is probably due to the partial loss of H$_2$O under vacuum, which results in higher concentrations for the remaining constituents. Analytical data are given in Table 2.

The empirical formula (based on V + Mg + Al + P + As = 6 and O = 25 atoms per formula unit) is $[(NH_4)_{3.11}K_{1.73}Na_{0.09}]_{\Sigma4.93}$ $[(V^{4+}_{1.92}Mg_{0.01}Al_{0.02})_{\Sigma1.95}O_2](C_2O_4)[(P_{3.94}As_{0.12})_{\Sigma4.06}O_{10.94}(OH)_{5.06}]\cdot$ 3H$_2$O. The simplified formula is $(NH_4,K)_5(V^{4+}O)_2(C_2O_4)$ $[PO_{2.75}(OH)_{1.25}]_4\cdot3H_2O$, which for 3 NH$_4$ and 2 K per formula unit (pfu) requires (NH$_4$)$_2$O 9.85, K$_2$O 11.88, VO$_2$ 20.91, P$_2$O$_5$

Table 2. Analytical data (wt.%) for davidbrownite-(NH$_4$).

Const.	Mean	Min.	Max.	S.D.	Probe standard
(NH$_4$)$_2$O	10.47	9.43	11.04	0.71	Cr$_2$N
K$_2$O	10.54	10.01	11.62	0.74	Sanidine
Na$_2$O	0.35	0.27	0.45	0.08	Albite
MgO	0.05	0.01	0.08	0.03	Diopside
Al$_2$O$_3$	0.12	0.10	0.16	0.03	Sanidine
VO$_2$	20.60	19.95	21.41	0.70	V metal
P$_2$O$_5$	36.17	35.34	37.17	0.76	Apatite
As$_2$O$_5$	1.76	1.40	2.12	0.31	Synthetic GaAs
C$_2$O$_3$*	9.33				
H$_2$O*	12.90				
Total	102.29				

* Based on the structure; S.D. – standard deviation.

35.79, C$_2$O$_3$ 9.08, H$_2$O 12.49, total 100 wt.%. The end-member formula is $(NH_4)_5(V^{4+}O)_2(C_2O_4)[PO_{2.75}(OH)_{1.25}]_4\cdot3H_2O$. The Gladstone–Dale compatibility (Mandarino, 2007) 1 − (K_p/K_c) is −0.032 in the range of excellent compatibility for the empirical formula.

X-ray crystallography and structure determination

Powder X-ray studies were done using a Rigaku R-Axis Rapid II curved imaging plate microdiffractometer with monochromatised Mo*K*α radiation. A Gandolfi-like motion on the φ and ω axes was used to randomise the sample. Observed *d* values and intensities were derived by profile fitting using *JADE 2010* software (Materials Data, Inc.). The powder data are presented in Table 3. Unit-cell parameters refined from the powder data using *JADE 2010* with whole pattern fitting are *a* = 10.370(13), *b* = 8.914(14), *c* = 13.470(14) Å, β = 92.70(2)° and *V* = 1244(3) Å^3.

Single-crystal X-ray studies were done using a Bruker D8 three-circle diffractometer equipped with a rotating anode generator (Mo*K*α X-radiation), multilayer optics and an APEX-II CCD area detector. The unit-cell dimensions were obtained by least-squares refinement of 3578 reflections with *I* > 10σ*I*. Systematically absent reflections are consistent with the space group *P*2$_1$/*c*. Empirical absorption corrections (*SADABS*; Sheldrick, 2015) were applied and equivalent reflections were merged. The structure was solved by direct methods using *SHELXS-2013* and the structure was refined to convergence using *SHELXL-2016* (Sheldrick, 2015). The partly occupied interstitial H$_2$O sites showed very anisotropic displacement behaviour; however, attempts to split the sites led to instability in the refinement and provided no additional useful crystal-chemical information. Data collection and refinement details are given in Table 4, atom coordinates and displacement parameters in Table 5, selected bond distances in Table 6 and a bond-valence analysis in Table 7. The crystallographic information files have been deposited with the Principal Editor of *Mineralogical Magazine* and are available as Supplementary material (see below).

Discussion of the structure

The structure consists of an ordered VO$_6$–(PΦ)$_4$–C$_2$O$_4$ structural unit (Φ = O and OH) and a disordered K–NH$_4$–H$_2$O interstitial complex. The H positions could not be located, and correct identification of O and OH anions bonded to the P atoms (in less typical fashion) was essential to complete an understanding of the structural unit, which then provided the necessary constraint to allow us to decipher the complex disordered interstitial region of the structure.

VO$_6$–(PΦ)$_4$–C$_2$O$_4$ structural unit

The V atoms are coordinated by six O atoms. Three of these O atoms, O3, O4 and O9, are shared with phosphate groups with V–O bond distances ranging from 1.969 to 2.026 Å, two O atoms, O1 and O2, are shared with the oxalate C$_2$O$_4$ group with longer V–O bonds of 2.272 and 2.058 Å, respectively, and one O atom, O11, forms a short vanadyl V = O bond of 1.601 Å. The long V–O bond of 2.272 Å is *trans* to the short vanadyl bond, giving a typical [1 + 4 + 1]-coordination (Schindler *et al.*, 2000). The interpreted 4$^+$ oxidation state of the V atoms is in agreement with the observed <$^{[6]}$V–O$_{eq}$> distance of 2.01 Å and derived bond-valence sum (Table 6) (Schindler *et al.*, 2000;

Table 3. Powder X-ray data (*d* in Å) for davidbrownite-(NH₄).

I_{obs}	d_{obs}	d_{calc}	I_{calc}	hkl
100	**10.39**	**10.3452**	**100**	**1 0 0**
50	**6.73**	**6.7568, 6.7360**	**9, 36**	**1 1 0, 0 0 2**
		6.1133	1	$\bar{1}$ 1 1
34	**5.97**	**5.9688**	**36**	**1 1 1**
33	**5.80**	**5.7666**	**25**	**$\bar{1}$ 0 2**
14	5.34	5.3761, 5.1726	12, 2	0 1 2, 2 0 0
11	4.69	4.7008, 4.4751, 4.4615, 4.2353	7, 1, 1, 1	1 1 2, 2 1 0, 0 2 0, 0 2 1
16	4.169	4.1975	7	2 1 1
16	4.069	4.0968, 4.0113	10, 4	1 2 0, 0 1 3
11	3.922	3.9394, 3.9000	5, 4	$\bar{1}$ 2 1, 1 2 1
35	**3.789**	**3.7973, 3.7925**	**6, 20**	**$\bar{2}$ 1 2, $\bar{1}$ 1 3**
12	3.696	3.6896, 3.6614	6, 6	1 1 3, 2 1 2
		3.3680	1	0 0 4
6	3.287	3.3003, 3.2541, 3.2465	1, 1, 2	$\bar{2}$ 2 1, 2 2 1, $\bar{1}$ 0 4
		3.2344	1	$\bar{2}$ 1 3
		3.2166	1	3 1 0
47	**3.160**	**3.1650, 3.1592, 3.1510**	**13, 5, 13**	**0 2 3, $\bar{3}$ 1 1, 0 1 4**
42	**3.104**	**3.1090, 3.0989**	**3, 25**	**2 1 3, 3 1 1**
35	3.043	3.0566, 3.0508, 3.0142	12, 6, 7	$\bar{2}$ 2 2, $\bar{1}$ 1 4, 3 0 2
		2.9996	1	1 2 3
44	**2.977**	**2.9844, 2.9519**	**23, 12**	**2 2 2, $\bar{3}$ 1 2**
16	2.906	2.9044, 2.8833	7, 2	0 3 1, $\bar{2}$ 0 4
14	2.855	2.8585	3	1 3 0
16	2.791	2.8035, 2.7891	8, 3	$\bar{1}$ 3 1, 1 3 1
		2.7209	1	0 3 2
12	2.689	2.6931, 2.6881	3, 2	$\bar{3}$ 2 1, 0 2 4
		2.6693	5	$\bar{3}$ 1 3
12	2.645	2.6555, 2.6251	7, 2	3 2 1, $\bar{1}$ 2 4
		2.6195	1	1 3 2
		2.5863	1	4 0 0
21	2.578	2.5794	14	0 1 5
		2.5612	1	$\bar{3}$ 2 2
		2.5432	1	$\bar{2}$ 3 1
		2.5219	1	2 3 1
		2.4976	1	3 2 2
9	2.487	2.4774	5	1 1 5
		2.4622	1	$\bar{4}$ 1 1
7	2.441	2.4522, 2.4266, 2.4240, 2.4216	2, 1, 2, 2	$\bar{4}$ 0 2, $\bar{2}$ 3 2, 4 1 1, $\bar{2}$ 2 4
6	2.380	2.3900, 2.3773	2, 2	2 3 2, $\bar{3}$ 1 4
		2.3701	1	$\bar{3}$ 2 3
		2.3645	2	$\bar{4}$ 1 2
		2.3504	1	2 2 4
		2.2701	2	$\bar{1}$ 2 5
12	2.234	2.2453, 2.2375, 2.2323, 2.2308, 2.2294	1, 1, 2, 1, 3	0 0 6, 4 2 0, $\bar{3}$ 3 1, 0 4 0, 0 3 4
		2.2215	1	$\bar{4}$ 2 1
		2.2152	1	$\bar{4}$ 1 3
		2.2107	1	3 3 1
11	2.198	2.1933	5	4 2 1
		2.1806	1	1 4 0
		2.1774	1	0 1 6
		2.1659	1	1 3 4
8	2.156	2.1555, 2.1490	2, 3	$\bar{3}$ 3 2, $\bar{4}$ 2 2
		2.1378	1	$\bar{2}$ 2 5
5	2.114	2.1102	2	$\bar{3}$ 1 5
		2.0805	1	$\bar{1}$ 4 2
6	2.0667	2.0690	3	5 0 0
		2.0378	1	$\bar{3}$ 3 3
		2.0351	1	$\bar{4}$ 2 3
		2.0306	2	$\bar{2}$ 4 1
7	2.0181	2.0156, 2.0065, 1.9969	1, 2, 1	5 1 0, $\bar{5}$ 1 1, 0 3 5
13	1.9656	1.9758, 1.9732, 1.9691, 1.9585, 1.9541	3, 1, 2, 3, 5	2 1 6, $\bar{1}$ 3 5, $\bar{1}$ 4 3, 4 1 4, 1 2 6
9	1.9399	1.9484, 1.9221	4, 3	1 3 5, 4 3 1

The strongest lines are given in bold.

Gagné and Hawthorne, 2015). The chemistry indicated the presence of minor As, which is presumed to occupy the P sites (~3% As occupancy). As such, the site occupancies of the P1 and P2 sites were refined with joint occupancy by P and As, resulting in a total of ~3.6% As at the two sites. (Table 5).

Pairs of VO₆ octahedra are linked by the bridging oxalate group, forming [V₂C₂O₁₂] dimers. Two of the O atoms (O3 and O4) of the P1 phosphate group are shared with the V atoms, with two P1 tetrahedra forming a double bridge between VO₆ octahedra. One O atom (O9) of the P2 phosphate group

Table 4. Data collection and structure refinement details for davidbrownite-(NH₄).

Crystal data	
Structural formula*	$(NH_4)_{2.83}K_{2.17}(V^{4+}O)_2(C_2O_4)[(P_{1.93}As_{0.07})O_{2.75}(OH)_{1.25}]_4\cdot3H_2O$
Crystal system, space group	Monoclinic, $P2_1/c$
Temperature (K)	293(2)
a, b, c (Å)	10.356(6), 8.923(5), 13.486(7)
β (°)	92.618(9)
V (Å³)	1244.9(12)
Z	2
Density (for above formula) (g·cm⁻³)	2.211
Absorption coefficient (mm⁻¹)	1.841
Data collection	
Crystal size (μm)	65 × 15 × 6
Diffractometer	Bruker D8 three-circle; multilayer optics; APEX–II CCD
X-ray radiation / source	MoKα (λ = 0.71073 Å) / rotating anode
F(000)	831.4
θ range for data collection (°)	2.74 to 27.51.
No. measured, independent and observed [$I_o > 2\sigma(I)$] reflections	36,607, 2867 [[R_{int} = 0.0681], 2062
Index ranges	−13 ≤ h ≤ 13, −11 ≤ k ≤ 11, −17 ≤ l ≤ 17
Refinement	
Refinement method	Full-matrix least-squares on F^2
Final R indices [$I > 2\sigma(I)$]	R_1 = 0.0524, wR_2 = 0.1261
R indices (all data)	R_1 = 0.0802, wR_2 = 0.1406
GoF on F^2	1.042
No. of parameters / restraints	210 / 3
Completeness to θ = 27.51°	100%
Largest diff. peak and hole (e^-/A³)	0.960 and −0.514

* Note that H atoms inferred from bond-valence considerations have been included in the structural formula even though they were not located in the structure refinement.
$R_{int} = \Sigma|F_o^2-F_o^2(mean)|/\Sigma[F_o^2]$. GoF = S = $\{\Sigma[w(F_o^2-F_c^2)^2]/(n-p)\}^{1/2}$. $R_1 = \Sigma||F_o|-|F_c||/\Sigma|F_o|$. $wR_2 = \{\Sigma[w(F_o^2-F_c^2)^2]/\Sigma[w(F_o^2)^2]\}^{1/2}$; $w = 1/[\sigma^2(F_o^2) + (aP)^2 + bP]$ where a is 0.0801, b is 0.9668 and P is $[2F_c^2 + Max(F_o^2,0)]/3$.

links to the V atom. The linkages between the VO₆ octahedra, oxalate groups and P1 phosphate groups gives a straight chain parallel to [010] that is decorated by P2 phosphate groups (Fig. 5).

The five anions of the phosphate groups that are not bonded to V atoms, O5, OH6, O7, OH8 and OH10, have incident bond-valence sums ranging from ∼1.2–1.5 valence units (vu) from their neighbouring cations (Table 7); however, bond-valence contributions from the disordered interstitial constituents are regarded as approximate. These five anions form three close

pairings between neighbouring phosphate groups OH8···OH8 (2.469 Å), OH6···O7 (2.500 Å) and OH10···O5 (2.573 Å), and very strong hydrogen bonding from OH groups is inferred (Fig. 6). In the absence of H positions, reliable hydrogen-bond valences can be determined from $O_D···O_A$ (D = hydrogen-bond donor; A = hydrogen-bond acceptor) distances (Brown, 2002). Our observed $O_D···O_A$ distances of 2.469, 2.500 and 2.573 Å are consistent with H-bond valences of 0.45, 0.40 and 0.35 vu, respectively (Brown, 2002), and donor valences (i.e. 1 − hydrogen-bond

Table 5. Atom positions and displacement parameters (Å²) for davidbrownite-(NH₄).

	x/a	y/b	z/c	U_{eq}	Refined occupancy	U^{11}	U^{22}	U^{33}	U^{23}	U^{13}	U^{12}
A1	0.3211(2)	0.3082(3)	0.33579(18)	0.0468(10)	N₀.₆₅₈(₈)K₀.₃₄₂(₈)	0.0494(16)	0.0484(16)	0.0427(16)	−0.0074(11)	0.0041(11)	−0.0092(11)
A2	0.93380(16)	0.17086(16)	0.30015(10)	0.0386(6)	K₀.₆₇₃(₇)N₀.₃₂₇(₇)	0.0617(11)	0.0317(9)	0.0225(8)	−0.0014(6)	0.0030(6)	−0.0016(7)
A3	0.4602(9)	0.0792(18)	0.5918(17)	0.157(8)	N₀.₄₂₉(₁₃)K₀.₀₇₁(₁₃)O₀.₂₁(₂)	0.056(6)	0.113(10)	0.30(2)	−0.020(11)	−0.017(7)	0.004(5)
OWA3	0.488(2)	0.161(3)	0.6397(13)	0.060(8)	O₀.₂₉(₂)☐₀.₇₁	0.063(12)	0.058(13)	0.057(11)	0.012(8)	−0.006(8)	0.035(10)
V	0.11410(7)	0.22455(8)	0.55967(5)	0.0196(2)	1	0.0235(4)	0.0162(4)	0.0195(4)	−0.0001(3)	0.0032(3)	−0.0008(3)
P1	0.82394(10)	0.07620(11)	0.56189(7)	0.0197(4)	P₀.₉₇₀(₄)As₀.₀₃₀(₄)	0.0246(6)	0.0154(5)	0.0196(6)	−0.0005(4)	0.0079(4)	−0.0008(4)
P2	0.33069(10)	0.48018(12)	0.61518(8)	0.0232(4)	P₀.₉₅₈(₄)As₀.₀₄₂(₄)	0.0252(6)	0.0244(6)	0.0206(6)	−0.0025(4)	0.0059(4)	−0.0048(4)
C	0.0167(4)	0.4900(4)	0.4456(3)	0.0192(8)	1	0.021(2)	0.017(2)	0.020(2)	−0.0009(15)	0.0016(16)	−0.0038(15)
O1	0.0755(3)	0.3725(3)	0.4245(2)	0.0234(6)	1	0.0278(16)	0.0212(15)	0.0215(15)	−0.0035(12)	0.0053(12)	0.0011(12)
O2	0.0185(3)	0.4075(3)	0.6134(2)	0.0229(6)	1	0.0315(16)	0.0196(14)	0.0178(15)	0.0007(11)	0.0046(12)	−0.0008(12)
O3	0.1939(3)	0.0886(3)	0.4651(3)	0.0327(8)	1	0.0357(18)	0.0190(15)	0.045(2)	−0.0077(14)	0.0193(15)	−0.0060(13)
O4	0.9409(3)	0.1463(3)	0.5147(2)	0.0226(6)	1	0.0261(15)	0.0196(15)	0.0223(15)	−0.0008(11)	0.0041(12)	−0.0032(12)
O5	0.2979(3)	0.8367(4)	0.4704(3)	0.0534(11)	1	0.0295(19)	0.041(2)	0.091(3)	0.035(2)	0.0149(19)	0.0104(16)
OH6	0.8463(4)	0.0828(5)	0.6762(2)	0.0522(11)	1	0.070(3)	0.072(3)	0.0155(17)	−0.0093(17)	0.0131(16)	−0.039(2)
O7	0.3250(3)	0.4614(4)	0.7267(2)	0.0376(8)	1	0.047(2)	0.044(2)	0.0222(17)	−0.0011(15)	0.0087(14)	0.0129(17)
OH8	0.4698(3)	0.5139(4)	0.5870(3)	0.0375(9)	1	0.0270(17)	0.050(2)	0.036(2)	−0.0125(16)	0.0076(14)	−0.0138(15)
O9	0.2831(3)	0.3390(4)	0.5595(2)	0.0298(7)	1	0.0251(16)	0.0303(17)	0.0345(18)	−0.0052(14)	0.0064(13)	−0.0061(13)
OH10	0.2410(3)	0.6163(4)	0.5834(3)	0.0394(9)	1	0.042(2)	0.0293(18)	0.048(2)	0.0107(16)	0.0074(16)	0.0016(15)
O11	0.1346(3)	0.1441(4)	0.6653(2)	0.0343(8)	1	0.0396(19)	0.0335(18)	0.0292(18)	0.0092(14)	−0.0029(14)	−0.0010(15)
OWa	0.676(2)	0.1282(17)	0.218(2)	0.102(8)	0.47(3)	0.153(15)	0.059(8)	0.089(14)	0.023(9)	−0.061(13)	−0.046(9)
OWb	0.6459(16)	0.119(2)	0.2722(15)	0.067(5)	0.42(3)	0.075(9)	0.074(9)	0.050(10)	0.008(8)	−0.028(7)	−0.003(7)
OWc	0.541(3)	0.123(3)	0.361(2)	0.025(9)	0.109(10)	0.029(16)	0.010(13)	0.033(17)	0.004(11)	−0.019(12)	−0.014(10)

Table 6. Selected interatomic distances (Å) in davidbrownite-(NH₄).

A1–OWc	2.82(3)	A2–O2	2.793(3)	A3–OWA3*	1.007(19)	V–O11	1.601(3)	P1–O3	1.524(3)	Weak hydrogen bonds	
A1–O7	2.821(5)	A2–O1	2.824(3)	A3–OWc*	1.91(3)	V–O3	1.969(3)	P1–O4	1.528(3)	OWA3–O5	2.727(19)
A1–OH8	2.844(4)	A2–OWa	2.867(17)	A3–O5	2.782(12)	V–O4	1.993(3)	P1–O5	1.528(4)	OWc–O5	2.78(2)
A1–O1	2.917(4)	A2–OH6	2.883(4)	A3–OWb	2.81(3)	V–O9	2.026(3)	P1–OH6	1.549(4)	OWA3–O9	2.825(15)
A1–OWa	2.947(18)	A2–O4	2.900(3)	A3–O9	2.976(13)	V–O2	2.058(3)	⟨P1–O⟩	1.532	OWc–O7	2.92(2)
A1–O11	2.965(4)	A2–O11	2.940(4)	A3–O5	3.152(18)	V–O1	2.272(3)			OWa–OH8	2.993(16)
A1–O3	2.972(4)	A2–OWb	3.023(16)	A3–O3	3.178(13)	⟨V–O⟩	1.987	P2–O7	1.517(3)		
A1–O9	3.072(4)	A2–OH10	3.100(4)	A3–A3§	3.00(5)			P2–OH8	1.536(3)	Strong hydrogen bonds	
A1–OWb	3.161(17)	A2–OH6	3.217(5)	A3–OWc	3.28(4)	C–O1	1.252(5)	P2–O9	1.536(3)	OH8–OH8	2.469(7)
A1–OWA3	3.234(18)	A2–O11	3.272(4)	A3–O7	3.398(15)	C–O2	1.255(5)	P2–OH10	1.577(4)	OH6–O7	2.500(5)
⟨A1–O⟩	2.975	⟨A2–O⟩	2.982	⟨A3–O⟩	3.072	C–C	1.533(8)	⟨P2–O⟩	1.542	OH10–O5	2.573(5)

* Not included in coordination; § A3 bonds to O occupying adjacent A3 site.

valence) of 0.55, 0.60 and 0.65 vu. Adding these respective H bond-valence contributions to the anions with the donor oxygens identified as OH8, OH6 and OH10 produces satisfactory bond-valence sums at the anions. In the extreme case of the very close approach between OH8 anions belonging to neighbouring separate P2 tetrahedra, the single H position is presumed to lie very close to the mid-point (i.e. a near-symmetrical hydrogen bond) and the hydrogen-bond valence ≈ donor bond valence. Thus, there are two OH8 anions pfu, but only a single associated H atom pfu, and the OH8 anion receives an average bond valence from the H atom of (0.45 + 0.55)/2 = 0.5 vu. It should be noted that two factors complicate rigorous bond-valence interpretations at these anions: (1) interstitial identity and position of the disordered (K, NH₄ and H₂O), which are presumably coupled to (2) the increased positional disorder observed for the anions themselves (i.e. larger displacement parameters for O5, OH6, O7, OH8 and OH10, Table 5). Similar strong hydrogen bonds between phosphate O atoms were noted in the structure of $Ca_2(NH_4)H_7(PO_4)_4 \cdot 2H_2O$ (Takagi et al., 1980). In davidbrownite-(NH₄), OH6 bonds to the P1 tetrahedron and OH8 and OH10 bond to the P2 tetrahedron giving $[P1O_3(OH)]_2$ and $[P2O_2(OH)O]_2$–H (or $[P2O_2(OH)O–H–O(OH)O_2P2]$ written symmetrically) pfu for a combined composition of $[PO_{2.75}(OH)_{1.25}]_4$

pfu. The chain structural units have the formula $\{(V^{4+}O)_2(C_2O_4)[PO_{2.75}(OH)_{1.25}]_4\}^{5-}$, which is balanced by five large monovalent cations pfu in the interstitial complex (see below).

NH₄–K–H₂O interstitial complex

Two fully occupied large-cation sites (A1 and A2) were refined with joint occupancy by N (NH₄) and K. The A1 site is occupied dominantly by NH₄ [$N_{0.658(8)}K_{0.342(8)}$] and the A2 site is occupied dominantly by K [$K_{0.673(7)}N_{0.327(7)}$]. Another site, A3, is interpreted as being partly occupied by both large cations and the O of an H₂O group, and this site is located ∼1 Å from a low occupancy O (H₂O) site (OWA3). To best fit the formula, the A3 site was refined as half occupied jointly by N and K (to provide a 1+ charge pfu) with the remaining site scattering accounted for by O, whose occupancy was linked to the OWA3 occupancy such that the total of the occupancies of the A3 and OWA3 sites is 1. The refined occupancies of the A3 and OWA3 sites are [$N_{0.429(13)}K_{0.071(13)}O_{0.21(3)}$] and $O_{0.29(3)}$, respectively. Note that the minor Na, indicated by the EPMA, is probably disordered over the A1, A2 and A3 sites. One additional H₂O group is split over sites (OWa/OWb/OWc), and the site-occupancies coupled to full occupancy. The combined A3 and OWA3 sites contribute one H₂O, and the combined (OWa/OWb/OWc) sites contribute two H₂O pfu, providing a total of three H₂O pfu. The complete structure is shown in Fig. 7.

Lewis acid–base considerations

Hawthorne (1985) first introduced the concept of binary structural representation in which a structure can be considered a combination of a strongly bonded 'structural unit' (usually anionic) and a weakly bonded 'interstitial complex'; this concept was

Table 7. Bond valences for davidbrownite-(NH₄) (not including hydrogen-bond contributions). Values are in valence units (vu).

	A1 (NH₄)	A2 (K)	A3×½→ (NH₄)	V	C	P1	P2	Σ
O1	0.15	0.14		0.26	1.44			1.99
O2		0.15		0.46	1.43			2.04
O3	0.13		0.08	0.59		1.28		2.04
O4		0.12		0.55		1.27		1.94
O5			0.22			1.27		1.42
			0.08					
OH6		0.12				1.21		1.38
		0.05						
O7	0.20		0.04				1.31	1.53
OH8	0.19						1.25	1.44
O9	0.10		0.13	0.50			1.25	1.92
OH10		0.07					1.13	1.20
O11	0.14	0.11		1.62				1.92
		0.05						
A3 (H₂O)			0.11					
OWA3	0.02							
OWa	0.07	0.06						
OWb	0.04	0.04	0.21					
OWc	0.03		0.06					
Σ	1.07	0.91	0.93	3.98	2.87	5.03	4.94	

Bond-valence parameters for NH₄⁺–O are from Garcia-Rodriguez et al. (2000); all others are from Gagné and Hawthorne (2015). The bond valences for the A1, A2 and A3 sites are based only on the dominant cation in each site, as noted. All of the bond valences for A3 contribute to only ½ of the listed values in the horizontal direction.
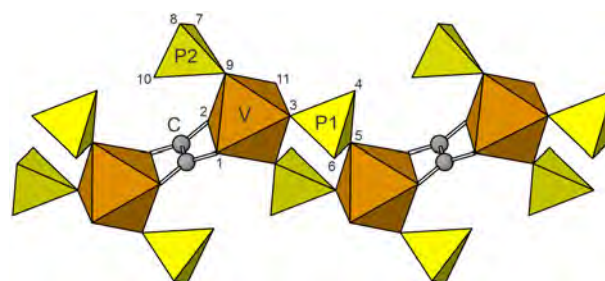

Fig. 5. The chain in the structure of davidbrownite-(NH₄), viewed down [10$\bar{1}$] with [010] horizontal. The O atoms are numbered.
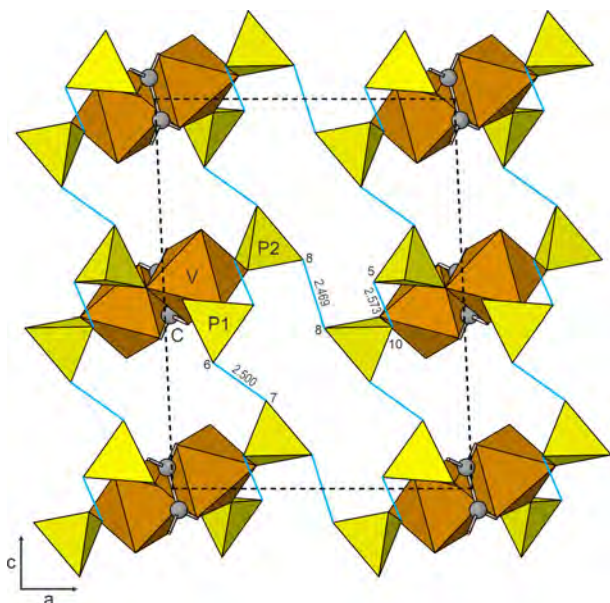
Fig. 6. The chains in the structure of davidbrownite-(NH$_4$), viewed down [010]. The strong hydrogen bonds (OH10–O5, OH6–O7 and OH8–OH8) are shown as blue lines. The O atoms participating in these bonds are labelled and their bond distances are shown. The NH$_4$, K and H$_2$O sites are omitted. The unit cell outline is shown with dashed lines.

expanded by Schindler and Hawthorne (2001) and Hawthorne and Schindler (2008). The structural unit is (usually) a complex oxyanion and can be characterised by its Lewis basicity. The interstitial complex is (usually) a complex cation and can be characterised by its Lewis acidity. The interaction between the structural unit and the interstitial complex can be examined using the 'principle of correspondence of Lewis acidity–basicity' (Hawthorne and Schindler, 2008). Calculation of the Lewis basicity of the structural unit requires the relation between the charge deficiency per anion of the structural unit and the average number
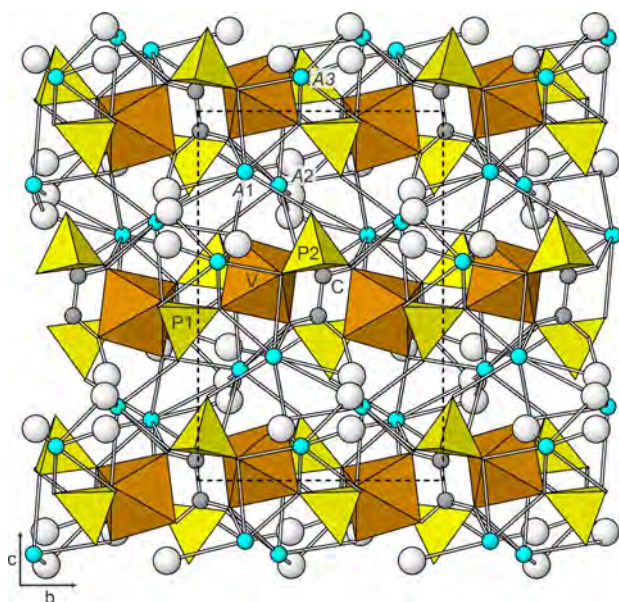

Fig. 7. The davidbrownite-(NH$_4$) structure viewed down [100]. The unit-cell outline is shown with dashed lines.

of bonds from the interstitial complex and adjacent structural units. This relation is derived from experimental structure data on particular oxysalt minerals, but is not yet available for phosphate minerals. In the absence of this relation, we may approximate the relation by specifying the average coordination number of a structural unit. Previous work used the coordination numbers [4] for silicate minerals and [3] for sulfate minerals (Hawthorne, 1997); the pentavalent nature of P suggests that we may use a coordination number intermediate between quadrivalent and hexavalent oxysalts: [3.5].

Let us write the formula of davidbrownite-(NH$_4$) as follows, where the structural unit is enclosed in square brackets and the interstitial complex is enclosed in curly brackets: $\{(NH_4, K)_5(H_2O)_3\}^{5+}[(V^{4+}O)_2(C_2^{3+}O_4)[PO_3(OH)]_4H]^{5-}$. The Lewis basicity of the structural unit is defined as the effective charge of the structural unit divided by the number of bonds needed by the structural unit. The number of anions in the structural unit is 22 and hence the number of bonds needed by the structural unit is $22 \times 3.5 = 77$. The number of bonds within the structural unit is $^{P-O}(4 \times 4) + {}^{V-O}(6 \times 2) + {}^{C-O}(2 \times 2) + {}^{H-O}(2 \times 5) = 42$, and hence the number of bonds needed by the structural unit from the interstitial complex is $77 - 42 = 35$. The charge on the structural unit is 5– and hence the Lewis basicity of the structural unit is $5 / 35 = 0.14$ vu. The interstitial complex, $\{(NH_4,K)_5(H_2O)_3\}^{5+}$, contains three cation sites, $A1$, $A2$ and $A3$, and four H$_2$O sites, OWa, OWb, OWc and OW$A3$. The $A1$, $A2$ and $A3$ sites have aggregate cation occupancies of 1.0, 1.0 and 0.5, and OWa, OWb, OWc have H$_2$O occupancies of 0.47, 0.42 and 0.11, respectively. We may calculate the Lewis acidity of the interstitial complex by dividing its aggregate charge by the number of bonds in the interstitial complex. The bond lengths involving the $A1$, $A2$ and $A3$ sites are listed in Table 6. However, the OW sites are all partly occupied and these partial occupancies have to be taken into account in calculating the coordination numbers; this leads to the following coordination numbers for $A1$, $A2$ and $A3$: [7], [8] and [5.4], respectively. Each of the H$_2$O groups is bonded to two cations and hence they are all non-transformer H$_2$O groups (Hawthorne, 2012) and will not affect the number of bonds from the interstitial complex to the structural unit. As the $A1$ and $A2$ sites are fully occupied and the $A3$ site is half-occupied (Table 5), this gives a total of $7 \times 2 + 8 \times 2 + 5.4 = 35.4$ bonds from the interstitial complex to the structural unit. Thus, the Lewis acidity of the interstitial complex is $5 / 35.4 = 0.14$ vu and the principle of correspondence of Lewis acidity–basicity holds. We have not made any predictions here, but we may draw some interesting conclusions. If the OWa, OWb and OWc sites were fully occupied, the Lewis acidity of the interstitial complex would be 0.11 vu, deviating somewhat from the principle of correspondence of Lewis acidity–basicity. This suggests that the partial occupancies of the H$_2$O sites are not random long-range disordered but are constrained by the Lewis basicity of the structural unit. Moreover, the partly occupied H$_2$O sites may couple to the type of interstitial cation occupying the locally associated $A1$, $A2$ and $A3$ sites. If this is the case, it suggests that davidbrownite-(NH$_4$) (and possibly many other associated secondary minerals) may be less disordered than their chemical formulae suggest.

Relation to other structures

While there are no other minerals with similar structures, a variety of phases have been synthesised that contain V^{4+} coordinated by both oxalate and phosphate anions (*cf.* Tsai *et al.*, 1999; Do *et al.*,

2000, 2001; Colin *et al.*, 2006; Nagarathinam *et al.*, 2012; Kouvatas *et al.*, 2017). Some of these phases, referred to as vanadyl oxalatophosphates, and particularly those with framework structures, have potential technological applications. We have not encountered any reports of vanadyl oxalatophosphate structures with the same chain topology as davidbrownite-(NH_4); however, similar linkages have been reported in several phases, in particular, $(NH_4)_2[VO(HPO_4)]_2(C_2O_4)\cdot 5H_2O$ (Do *et al.*, 2000) and $Na_2[(VO)_2(HPO_4)_2C_2O_4]\cdot 2H_2O$ (Colin *et al.*, 2006), both of which have layer structures. A vanadyl oxalatophosphite chain with topology similar to that of the chain in davidbrownite-(NH_4) was reported in $(NH_4)_2(VOHPO_3)_2C_2O_4\cdot 2.9H_2O$ (Kouvatas *et al.*, 2017).

References

Beran A., Armstrong J. and Rossman G.R. (1992) Infrared and electron microprobe analysis of ammonium ions in hyalophane feldspar. *European Journal of Mineralogy*, **4**, 847–850.

Brown I.D. (2002) *The Chemical Bond in Inorganic Chemistry. The Bond Valence Model.* Oxford University Press, Oxford, UK.

Brown I.D. (2016) *The Chemical Bond in Inorganic Chemistry: The Bond Valence Model.* 2nd Edition. Oxford University Press, Oxford.

Chukanov N.V., Pekov I.V., Olysych L.V., Zubkova N.V. and Vigasina M.F. (2011) Crystal chemistry of cancrinite-group minerals with an *AB*-type framework: A review and new data. II. IR spectroscopy and its crystal-chemical implications. *The Canadian Mineralogist*, **49**, 1151–1164.

Colin J.F., Bataille T., Ashbrook S.E., Audebrand N., Le Pollès L., Pivan J.Y. and Le Fur E. (2006) $Na_2[(VO)_2(HPO_4)_2C_2O_4]\cdot 2H_2O$: crystal structure determination from combined powder diffraction and solid-state NMR. *Inorganic Chemistry*, **45**, 6034–6040.

Do J., Bontchev R.P. and Jacobson A.J. (2000) A hydrothermal investigation of the ½V_2O_5–$H_2C_2O_4$/H_3PO_4/NH_4OH system: synthesis and structures of $(NH_4)VOPO_4\cdot 1.5H_2O$, $(NH_4)_{0.5}VOPO_4\cdot 1.5H_2O$, $(NH_4)_2[VO(H_2O)_3]_2[VO(H_2O)][VO(PO_4)_2]_2\cdot 3H_2O$, and $(NH_4)_2[VO(HPO_4)]_2(C_2O_4)\cdot 5H_2O$. *Inorganic Chemistry*, **39**, 3230–3237.

Do J., Bontchev R.P. and Jacobson A.J. (2001) Vanadyl oxalatophosphate compounds $(C_2H_{10}N_2)[VO(HPO_4)]_2(C_2O_4)$ and $(CH_6N_3)_2[[VO(HPO_4)]_2(C_2O_4)]$ and their thermal transformation to $(VO)_2P_2O_7$ via VOHPO_4. *Chemistry of Materials*, **13**, 2601–2607.

Edwards H.G.M., Farwell D.W., Rose S.J. and Smith D.N. (1991) Vibrational spectra of copper(II) oxalate dihydrate, $CuC_2O_4\cdot 2H_2O$, and dipotassium bis-oxalato copper(II) tetrahydrate, $K_2Cu(C_2O_4)_2\cdot 4H_2O$. *Journal of Molecular Structure*, **249**, 233–243.

Frost R.L. and Weier M.L. (2003) Raman spectroscopy of natural oxalates at 298 and 77 K. *Journal of Raman Spectroscopy*, **34**, 776–785.

Gagné O.C. and Hawthorne F.C (2015) Comprehensive derivation of bond-valence parameters for ion pairs involving oxygen. *Acta Crystallographica*, **B71**, 562–578.

García-Rodríguez L., Rute-Pérez Á., Piñero J.R. and González-Silgo C. (2000) Bond-valence parameters for ammonium-anion interactions. *Acta Crystallographica*, **B56**, 565–569.

Gunter M.E., Bandli B.R., Bloss F.D., Evans S.H., Su S.C. and Weaver R. (2004) Results from a McCrone spindle stage short course, a new version of EXCALIBR, and how to build a spindle stage. *The Microscope*, **52**, 23–39.

Hammer V.M.F., Libowitzky E. and Rossman G.R. (1998) Single-crystal IR spectroscopy of very strong hydrogen bonds in pectolite, $NaCa_2[Si_3O_8(OH)]$, and serandite, $NaMn_2[Si_3O_8(OH)]$. *American Mineralogist*, **83**, 569–576.

Hawthorne F.C. (1985) Towards a structural classification of minerals: the $^{vi}M^{iv}T_2\emptyset_n$ minerals. *American Mineralogist*, **70**, 455–473.

Hawthorne F.C. (1997) Structural aspects of oxide and oxysalt minerals. Pp. 373–429 in: *Modular Aspects of Minerals* (S. Merlino, editor). European Mineralogical Union Notes in Mineralogy, Vol. **1**, Eötvös University Press, Budapest, Hungary.

Hawthorne F.C. (2012) A bond-topological approach to theoretical mineralogy: crystal structure, chemical composition and chemical reactions. *Physics and Chemistry of Minerals*, **39**, 841–874.

Hawthorne F.C. and Schindler M. (2008) Understanding the weakly bonded constituents in oxysalt minerals. *Zeitschrift für Kristallographie*, **223**, 41–68.

Kampf A.R., Cooper M.A., Nash B.P, Cerling T., Marty J., Hummer D.R., Celestian A.J., Rose T.P. and Trebisky T.J. (2017) Rowleyite, $[Na(NH_4, K)_9Cl_4][V_2^{5+,4+}(P,As)O_8]_6\cdot n[H_2O,Na,NH_4,K,Cl]$, a new mineral with a mesoporous framework structure. *American Mineralogist*, **102**, 1037–1044.

Kampf A.R., Celestian A.J., Nash B.P. and Marty J. (2019a) Phoxite, $(NH_4)_2Mg_2(C_2O_4)(PO_3OH)_2(H_2O)_4$, the first phosphate-oxalate mineral. *American Mineralogist*, **104**, 973–979.

Kampf A.R., Cooper M.A., Rossman G.R., Nash B.P., Hawthorne F.C. and Marty J. (2019b) Davidbrownite, IMA 2018-129. CNMNC Newsletter No. 47, February 2019, page 146; *Mineralogical Magazine*, **83**, 143–147.

Kouvatas C., Alonzo V., Bataille T., Le Pollès L., Roiland C., Louarn G. and Le Fur E. (2017) Synthesis, crystal structure of the ammonium vanadyl oxalatophosphite and its controlled conversion into catalytic vanadyl phosphates. *Journal of Solid State Chemistry*, **253**, 73–77.

Libowitzky E. (1999) Correlation of O–H stretching frequencies and O–H···O hydrogen bond lengths in minerals. *Monatshefte für Chemie*, **130**, 1047–1059.

Mandarino J.A. (2007) The Gladstone–Dale compatibility of minerals and its use in selecting mineral species for further study. *The Canadian Mineralogist*, **45**, 1307–1324.

Nagarathinam M., Saravanan K., Phua E.J.H., Reddy M.V., Chowdari B.V.R. and Vittal J.J. (2012) Redox-active metal-centered oxalato phosphate open framework cathode materials for lithium ion batteries. *Angewandte Chimie International Edition*, **51**, 5866–5870.

Orive J., Sivasamy R., Fernández de Luis R., Mosquera E. and Arriortua M.I. (2018) $K_2Mn_2^{II}(H_2O)_2C_2O_4(HPO_3)_2$: a new 2D manganese(II) oxalatophosphite with double-layered honeycomb sheets stabilized by potassium ions. *CrystEngComm*, **20**, 301–311.

Pouchou J.-L. and Pichoir F. (1991) Quantitative analysis of homogeneous or stratified microvolumes applying the model "PAP." Pp. 3l–75 in: *Electron Probe Quantitation* (K.F.J. Heinrich and D.E. Newbury, D.E., editors). Plenum Press, New York.

Sheldrick G.M. (2015) Crystal structure refinement with *SHELX*. *Acta Crystallographica*, **C71**, 3–8.

Schindler M., Hawthorne F.C. and Baur W.H. (2000) Crystal chemical aspects of vanadium: polyhedral geometries, characteristic bond valences, and polymerization of (VO_n) polyhedra. *Chemistry of Materials*, **12**, 1248–1259.

Schindler M. and Hawthorne F.C. (2001) A bond-valence approach to the structure, chemistry, and paragenesis of hydroxyl-hydrated oxysalt minerals. I. Theory. *The Canadian Mineralogist*, **9**, 1225–1242.

Takagi S., Mathew M. and Brown W.E. (1980) phosphate ion with three 'symmetric' hydrogen bonds: The structure of $Ca_2(NH_4)H_7(PO_4)_4\cdot 2H_2O$. *Acta Crystallographica*, **B36**, 766–771.

Tsai Y.-M., Wang S.-L., Huang C.-H. and Lii K.-H. (1999) Synthesis and structural characterization of the first organically templated vanadyl(IV) arsenato- and phosphato-oxalates: $(C_4H_{12}N_2)[VO(C_2O_4)HXO_4]$ (X = As, P). *Inorganic Chemistry*, **38**, 4183–4187.

Wilson W.E., and Miller D.K. (1974) Minerals of the Rowley mine. *Mineralogical Record*, **5**, 10–30.